Polyimide-Surface-Modified Silica Tubes: Preparation and Cryogenic Properties

Yihe Zhang,*[,†,‡] Yuanqing Li,[#] Guangtao Li,[⊥] Haitao Huang,[‡] H. L. W. Chan,[‡] Walid A. Daoud,[§] John H. Xin,[§] and Laifeng Li*[,#]

School of Materials Science and Technology, China University of Geosciences, Beijing 100083, China, Department of Applied Physics and Materials Research Centre, The Hong Kong Polytechnic University, Hong Kong, China, Technical Institute of Physics and Chemistry, Chinese Academy of Sciences, Beijing 100080, China, Department of Chemistry, Tsinghua University, Beijing 100084, China, and Nanotechnology Centre, Institute of Textile and Clothing, The Hong Kong Polytechnic University, Hong Kong, China

Received October 25, 2006. Revised Manuscript Received February 10, 2007

The silica tubes were synthesized by template self-assembly from D,L-tartaric acid and hydrolysis of tetraethoxysilane (TEOS), and their surfaces were modified by a 3-aminopropyltriethoxysilane coupling agent. Thereafter, a series of polyimide (PI)-surface modified silica tube (ST) hybrid films was prepared from PMDA-ODA in *N*,*N*-dimethylacetamide as a solvent using an in situ polymerization process combined with ultrasonic dispersion and multistep curing. The resulting silica tubes and the hybrid films were characterized using XRD, SEM, TEM, FTIR, and UV−vis. The cryogenic mechanical properties at 77 K and dynamic mechanical properties of the hybrid films were studied. The results indicated that the strength, modulus, and failure strain of the hybrid films were all increased compared with those of the pure PI film when the silica tube content was at 1−3 wt %. The cryogenic tensile strength and modulus were generally higher than those at room temperature, whereas the cryogenic failure strain was lower than that at room temperature. The elastic modulus of the hybrid films exhibited a monotonically increasing trend. The cryogenic failure strain of hybrid films with 1−3 wt % silica tube contents was greater than with 15 wt %, indicating a good ductility at 77 K. The glass-transition temperature of the hybrid films increased with the increase in silica tube content.

1. Introduction

Polyimide (PI) films have been widely used in many applications such as microelectronics and aerospace because of their excellent thermal stability, chemical resistance, mechanical properties, low thermal expansion coefficient, and low dielectric constant. However, their mechanical and thermal properties need to be further enhanced in cryogenic and high-temperature applications. One possible solution is to employ polyimide−inorganic nanocomposites that possess novel properties through careful design of the nanocomposites. Several classes of polyimide hybrid materials have been reported in the literature.[1−13] Improved thermal stability, optical properties, mechanical properties, gas barrier properties, and water absorption retardation behavior were shown in comparison with the pure polyimide films. In recent years, with the rapid developments in spacecraft and superconductive cables technologies, cryogenic properties of PI hybrid films have attracted many research efforts. Polyimide hybrid films are potential insulating materials for the International Thermonuclear Experimental Reactor (ITER) insulating system and the TOKAMAK system. These cryogenic systems have high demands for insulating materials.[14,15] The requirements for polyimide films in these special applications are extremely severe, and PI hybrid films with enhanced cryogenic mechanical properties are needed. Cryogenic mechanical behaviors of materials are generally very different from those at room temperature. The mechanical properties obtained from room temperature cannot be extrapolated to a cryogenic case.

* To whom correspondence should be addressed. E-mail: zyh@cugb.edu.cn (Y.Z.); lfli@cl.cryo.ac.cn (L.L.).
† China University of Geosciences.
‡ Department of Applied Physics and Materials Research Centre, The Hong Kong Polytechnic University.
# Chinese Academy of Sciences.
⊥ Tsinghua University.
§ Institute of Textile and Clothing, The Hong Kong Polytechnic University.

(1) Yano, K.; Usuki, A.; Okada, A. *J. Polym. Sci., Part A: Polym. Chem.* **1997**, *35*, 2289.
(2) Tsai, M. H.; Whang, W. T. *Polymer* **2001**, *42*, 4197.
(3) Magaraphan, R.; Lilayuthalert, W.; Sirivat, A.; Schwank, J. W. *Comput. Sci. Technol.* **2001**, *61*, 1253.
(4) Chiang, P. C.; Whang, W. T.; Tsai, M. H.; Wu, S. C. *Thin Solid Films* **2004**, *447*, 359.
(5) Tyan, H. L.; Liu, Y. C.; Wei, K. H. *Chem. Mater.* **1999**, *11*, 1942.
(6) Huang, J. C.; Zhu, Z. K.; Ma, X. D.; Qian, X. F.; Yin, J. *Mater. Sci. Eng.* **2001**, *36*, 871.
(7) Tyan, H. L.; Leu, C. M.; Wei, K. H. *Chem. Mater.* **2001**, *13*, 222.
(8) Morgan, A. B.; Gilman, J. W.; Jackson, C. L. *Macromolecules* **2001**, *34*, 2735.
(9) Tyan, H. L.; Wei, K. H.; Hsieh, T. E. *J. Polym. Sci., Part B: Polym. Phys.* **2000**, *38*, 2873.
(10) Jiang, L. Y.; Leu, C. M.; Wei, K. H. *Adv. Mater.* **2002**, *14*, 426.
(11) Chang, C. C.; Chen, W. C. *Chem. Mater.* **2002**, *14*, 4242.
(12) Ahmad, Z.; Mark, J. E. *Chem. Mater.* **2001**, *13*, 3320.
(13) Shang, X. Y.; Zhu, Z. K.; Yin, J.; Ma, X. D. *Chem. Mater.* **2002**, *14*, 71.
(14) Broadbend, A. J.; Crozier, J.; Smith, K. D.; Street, A. J.; Wiatrzy, J. M. *Cryogenics* **1995**, *35*, 701.
(15) Rohrhofer, K. B.; Humer, K.; Weber, H. W. *Cryogenics* **2002**, *42*, 265.

10.1021/cm062540m CCC: $37.00
Published on Web 03/20/2007

Recently, studies on one-dimensional tubular nanomaterials such as carbon nanotubes,[16−22] SiO_2,[23−27] TiO_2,[28−30] V_2O_5,[31] and MoS_2[32] have been reported. These new materials have larger specific surface areas, high aspect ratios, and hollow structures, which are suitable for reinforcement fillers, chemical probes, sensors, hydrogen storages, displays[17−22] and templates to grow other nanomaterials.

Although cryogenic mechanical properties of pure PI films and PI−Montmorillonite (MMT) nanocomposite films have been studied previously,[33,34] it is quite difficult to reach a high level of exfoliation of MMT in the PI film. Mechanical properties of PI−silica particles and dielectric properties of PI−silica tubes have also been reported.[13,35,36] However, no report has been published on the cryogenic mechanical properties of the silica-tube-modified polymer nanocomposites. As illustrated in Figure 1, the shape of silica tubes with high aspect ratio is different from those of spherical silica particles and layered silicates such as MMT and mica, mimicking that of sand, steel tube, and other fillers in concrete. Because of the hollow and high aspect ratio of the tubular silica structures, in analogy to carbon nanotubes, the silica tubes are modified with an amino coupling agent, and improved dispersion with minimum possible aggregation in the PI matrix as compared with MMT layer counterparts is observed. Improved dispersion of ST fillers in the PI matrix leads to better mechanical properties at room and cryogenic temperatures.

In the present investigation, we report the employment of silica tubes as reinforcement fillers to incorporate into the polyimide matrix in an attempt to improve the cryogenic mechanical properties of the hybrid films. The silica tubes were synthesized by template self-assembly, and their surfaces were modified by a coupling agent. A series of novel PI−ST hybrid films were prepared by an in situ polymerization process combined with ultrasonic dispersion and multistep curing. Figure 2 illustrates the reaction scheme for preparing polyimide−silica tube (amino-modified) hybrid films. The prepared silica tube and the hybrid films were characterized using XRD, SEM, TEM, FTIR, and UV−vis. The dependence of cryogenic mechanical properties on silica tube content and dependence of dynamic mechanical property on temperature and silica tube content of the hybrid films are discussed.

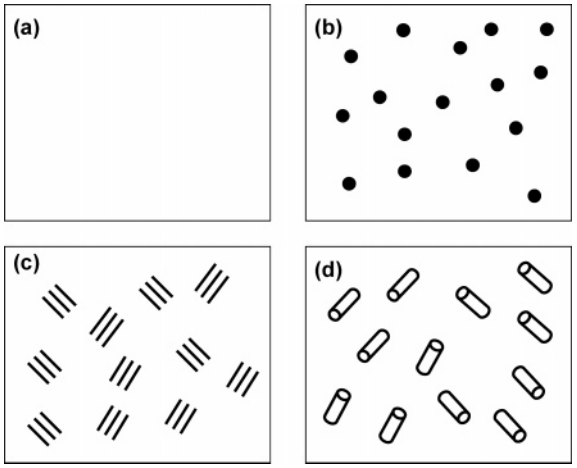

Figure 1. Schemes of different fillers and dispersive behavior in polymer matrix.

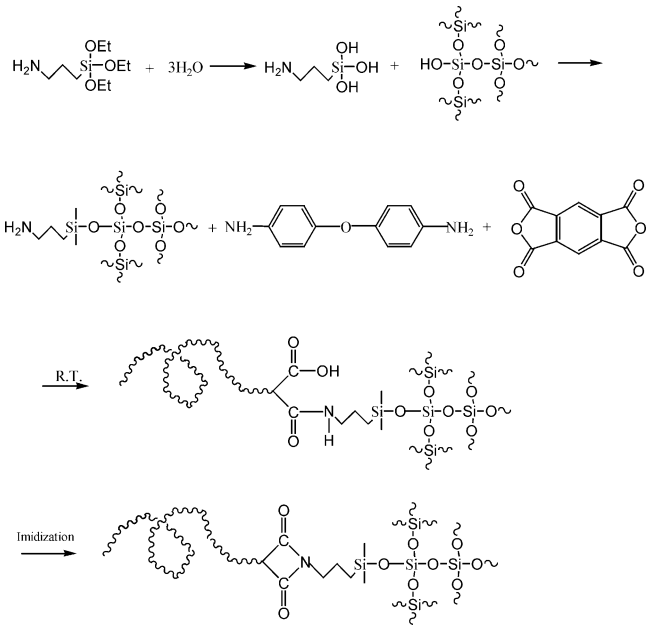

Figure 2. Reaction scheme for preparing polyimide−silica tube (amino-modified) hybrid films.

2. Experimental Section

2.1. Materials. Pyromellitic dianhydride (PMDA, 99%) and 4,4′-oxidianiline (ODA, 99%) were of chemical reagent grade and purchased from Tianjin Chemicals Co. (Tianjin, China); they were further purified by sublimation before use. *N*,*N*-Dimethylacetamide (DMAc, analytical reagent grade), 3-aminopropyltriethoxysilane (APTEOS, chemical reagent grade, 98$^+$%), and D,L-tartaric acid (analytical reagent grade) were purchased from Beijing Reagent

(16) Iijima, S. *Nature* **1991**, *354*, 56.
(17) Kong, J.; Franklin, N. R.; Zhou, C.; Chapline, M. G.; Peng, S.; Cho, K.; Dai, H. *Science* **2000**, *287*, 622.
(18) Liu, C.; Fan, Y. Y.; Liu, M.; Cong, H. T.; Cheng, H. M.; Dresselhaus, M. S. *Science* **1999**, *286*, 1127.
(19) Ajayan, P. M. *Chem. Rev.* **1999**, *99*, 1787.
(20) Wong, S. S.; Joselevich, E.; Woolley, A. T.; Cheung, C. L.; Lieber, V. M. *Nature* **1998**, *394*, 52.
(21) Park, C.; Ounaies, Z.; Watson, K. A.; Crooks, R. E., Jr.; Smith, J.; Lowther, S. E.; Connell, J. W.; Siochi, E. J.; Harrison, J. S.; St. Clair, T. L. *Chem. Phys. Lett.* **2002**, *364*, 303.
(22) Qu, L.; Lin, Y.; Hill, D. E.; Zhou, B.; Wang, W.; Sun, X.; Kitaygorodskiy, A.; Suarez, M.; Connel, J. W.; Allard, L. F.; Sun, Y. P. *Macromolecules* **2004**, *37*, 6055.
(23) Stephanie, T. R.; Oliver, S. *J. Am. Chem. Soc.* **2003**, *125*, 4338.
(24) Satishkumar, B. C.; Govindaraj, A. *J. Mater. Res.* **1997**, *12*, 604.
(25) Harada, M.; Adachi, M. *Adv. Mater.* **2000**, *12*, 839.
(26) Miyaji, F.; Davis, S. A.; Charmant, J. P. H.; Mann, S. *Chem. Mater.* **1999**, *11*, 3021.
(27) Nakamura, H.; Matsui, Y. *J. Am. Chem. Soc.* **1995**, *117*, 2651.
(28) Kasuga, T.; Hiramatsu, M.; Hoson, A.; Kekino, T.; Niihara, K. *Langmuir* **1998**, *14*, 3160.
(29) Imai, H.; Takei, Y.; Shimizu, K.; Matsuda, M.; Hirashima, H. *J. Mater. Chem.* **1999**, *9*, 2971.
(30) Caruso, R. A.; Schattka, J. H.; Greiner, A. *Adv. Mater.* **2001**, *13*, 1577.
(31) Spahr, M. E.; Stoschitizki, R.; Bitterci, P.; Nesper, R. *Angew. Chem., Int. Ed.* **1998**, *37*, 1263.
(32) Tdldman, Y.; Wasserman, E.; Srolovitz, D. J.; Tenne, R. *Science* **1995**, *267*, 222.
(33) Yamaoka, H.; Miyata, K.; Yano, O. *Cryogenics* **1995**, *35*, 787.
(34) Zhang, Y. H.; Wu, J. T.; Fu, S. Y.; Yang, S. Y.; Li, Y.; Fan, L.; Li, R. K. Y.; Li, L. F.; Yan, Q. *Polymer* **2004**, *45*, 7579.
(35) Zhang, Y. H.; Li, Y.; Fu, S. Y.; Xin, J. H.; Daoud, W. A.; Li, L. F. *Polymer* **2005**, *46*, 8373−8378.
(36) Zhang, Y. H.; Lu, S. G.; Li, y. q.; Dang, z. m.; Xin, J. H.; Fu, S. Y.; Li, G. T.; Guo, R. R.; Li, L. F. *Adv. Mater.* **2005**, *17*, 1056−1059.

Co. (Beijing, China), and DMAc was dried over molecular sieves before use. Tetraethoxysilane (TEOS, chemical reagent grade) was obtained from Tianjin Chemicals Co. and used without further purification. Common reagents, such as ammonia and ethanol, were used without any further purification.

2.2. Preparation of Silica Tubes by Self-Assembly. The silica tubes were synthesized by hydrolyzing the TEOS using D,L-tartaric acid as a template according to the literature. For the preparation of silica tubes, 0.73 g of TEOS was added into 5 mL of ethanol containing 0.02 g of d,L-tartaric acid and 0.06 g of distilled water, and the mixture solution was allowed to stand for 30 min. Subsequently, 2 mL of 28% aqueous NH_3 was added to the solution and allowed to stand for 30 min. The product was washed with a large amount of water on a 0.2 μm membrane filter and dried at room temperature.

2.3. Preparation of Pure Polyimide (PMDA-ODA) Film. Pure PI film was prepared in parallel to the PI−silica tube hybrid films for comparison purposes. In a typical example, 6.5439 g (30 mmol) of PMDA, 6.0071 g (30 mmol) of ODA, and 70 g of DMAc were added to a 150 mL flask. The molar ratio of dianhydride to diamine was 1:1, and the total concentration of the reaction solution was 12 wt %. The system was equipped with a nitrogen inlet and mechanical stirrer. The mixture was stirred at room temperature under nitrogen for about 5 h until the mixture became viscous. The pure polyimide film was prepared by casting the poly(amic acid) (PAA) solution onto a glass plate. After the film had been dried at room temperature for 1 h, it was heated for imidization at 80, 120, and 150 °C for 1 h each and at 250 and 300 °C for 0.5 h each to obtain a yellow colored transparent film.

2.4. Preparation of the PI−ST Hybrid Films. The hybrid films were prepared using an ultrasonic dispersion and in situ polymerization reaction followed by casting and multistep thermal curing. The synthetic reaction scheme was shown in Figure 2. Typically, in a beaker, a predetermined quantity of silica tubes and 3-aminopropyltriethoxysilane coupling agent were added to DMAc solvent. After the solution was stirred for 12 h, it was further dispersed in an ultrasonic bath for 30 min to obtain surface-modified silica tubes. The mixture and ODA were added to a flask equipped with nitrogen inlet and mechanical stirrer. After ODA was dissolved in DMAc, PMDA was added under nitrogen protection with stirring. After 10 h, the resulting homogeneous solution was then cast onto a glass plate. The following multistep thermal curing process was the same as that for the pure PI film, and finally a series of hybrid films were obtained.

2.5. Characterization. Scanning electron microscope (SEM) photographs of the silica tube as well as the fracture surfaces of films at room and cryogenic temperatures were taken with a HITACHI S-4300 SEM. Transmission electron microscope (TEM) measurement was performed with a HITACHI 800 TEM. The X-ray diffractometer (XRD) patterns of PI−ST nanocomposite films were obtained by a Siemens X-ray diffractometer Model D500 using Cu Kα radiation source (λ = 0.154 nm), operated at 40 kV and 30 mA. The infrared spectra (FT−IR) of PI and PI−ST hybrid films were measured with FT−IR 16 PC from Perkin Elmer. The ultraviolet−visible (UV−vis) light transmissions of PI and PI−ST hybrid films were measured with a Lambda 2S UV−vis spectrometer from Perkin Elmer. The tensile properties of PI and PI−ST hybrid films at cryogenic (77 K) and room temperatures were measured by an Instron 1122 tensile tester with a special liquid temperature chamber at the loading rate of 2 mm/min. The dimensions of film specimens were 10 mm × 120 mm. The thickness of films was 25−38 μm, and the specimens were cut from free films. The gauge length was 50 mm. More than six samples were tested for each composition. Dynamic mechanical measurement was performed by means of a DMA 2980 from TA Instruments (nitrogen flux; frequency, 10 Hz; temperature range, −150 to 500 °C; heating rate, 5 °C /min).

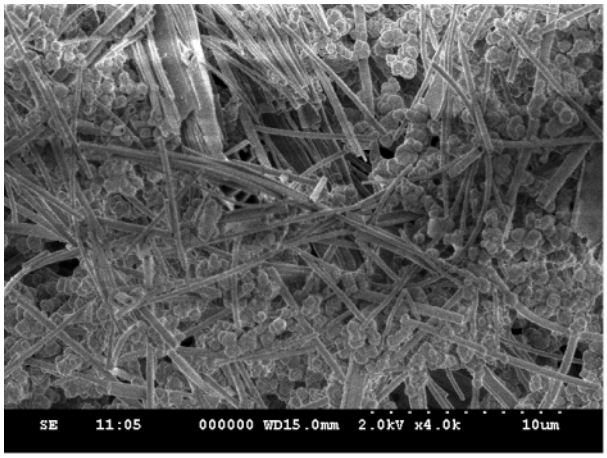

(a)

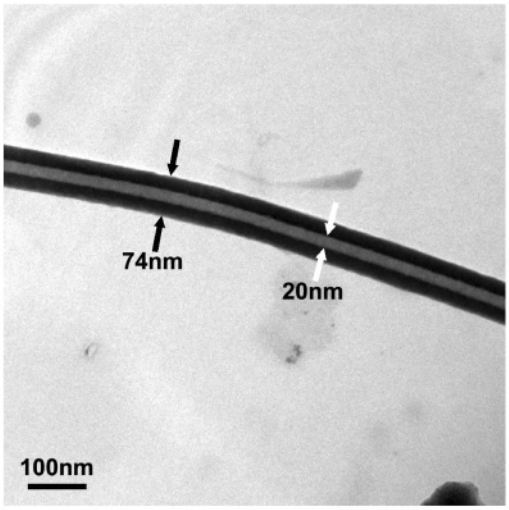

(b)

Figure 3. (a) SEM photograph and (b, c) TEM photographs of silica tubes.

3. Results and Discussion

3.1. SEM and TEM Characterization of Silica Tubes. Figure 3 showed the SEM and TEM photographs of silica tubes (images a and b of Figure 3, respectively). It was seen from the SEM photograph that the silica tubes were formed in the presence of ammonium D,L-tartrate crystal templates. The outer and inner sizes in cross-section length of the tubes are about 70−530 and 20−320 nm, respectively, and the length is 40−400 μm. Around the tubes, there were small quantities of silica particles with size of tens to hundreds of nanometers in diameter. In the process of forming silica tubes, the TEOS was hydrolyzed into silica and then gradually attached onto the ammonium D,L-tartrate templates to form the silica tubes. The formation of ammonium D,L-tartrate templates and the deposition of silica onto the side faces of the templates were almost simultaneous when the ammonia was added to the solution.[26] Because the crystal templates could not grow further when silica starts to deposit on them, the width of the tube would increase with increasing ratio of the crystal template growth rate along the width

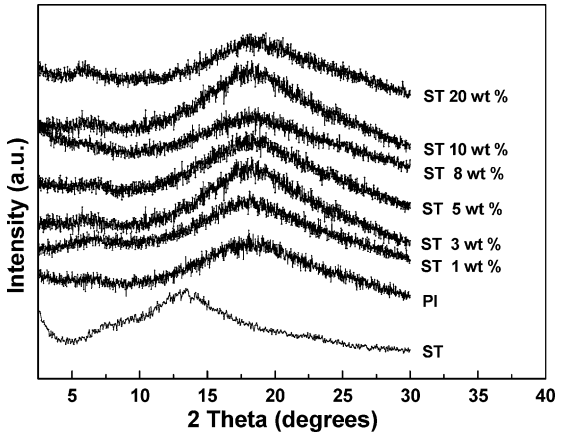

Figure 4. XRD patterns of silica tube, PI, and PI−silica tube hybrid films.

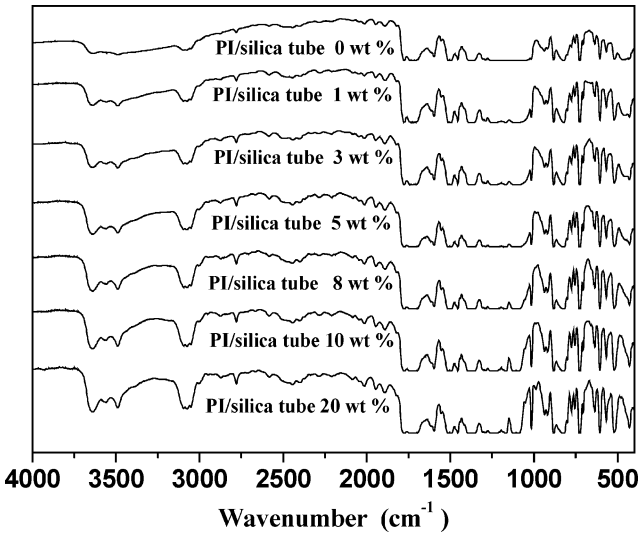

Figure 5. FT−IR spectrum of PI and PI−ST hybrids.

direction to the TEOS deposition rate. Hence, the width of the silica tube changed with different reaction conditions, e.g., different acid and TEOS concentrations. This phenomenon could also be explained in terms of the change in the rates of the template growth and/or silica deposition.[26] On the other hand, the formation of hollow silica tubes in the presence of D,L-tartrate templates was attributed to no silica deposition on the end faces of the crystal templates.

3.2. XRD, FTIR, UV−Vis Characterization. Figure 4 illustrated the XRD patterns of silica tube, pure PI, and PI−ST hybrid films in the 2θ range of 1−30°. No clear XRD peaks appeared except for a broad amorphous band for the silica tube at $2\theta = 5-25°$ (the top is around 13°) and a broad amorphous peak for PI at $2\theta = 5-30°$ (the top is around 18°). The amorphous band of silica tube could not been found in the XRD pattern of the PI/ST hybrids. This indicated that the silica tubes were chemically bonded with PI by the coupling agent, and they could be detected by means of X-ray diffraction.

Figure 5 showed the FTIR spectra of the prepared pure PI and PI−ST hybrid films. The characteristic absorption bands of the imide group can be observed at 727, 1380, and 1780 cm^{-1} for all samples. The main difference between pure PI and PI−silica tube hybrid films is the absorption bands around 1014 and 428 cm^{-1}. These two absorption bands were

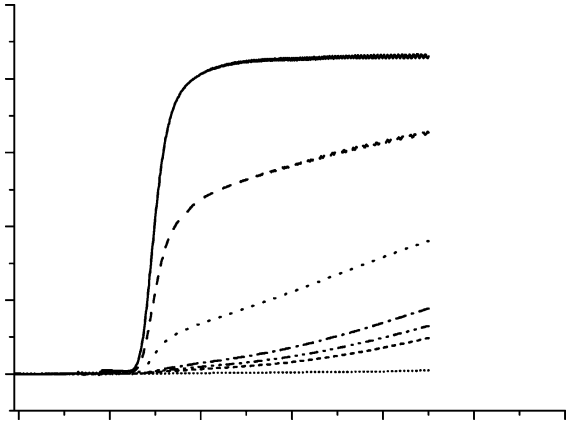

Figure 6. UV−vis transmission of PI and PI−ST hybrid films.

ascribed to Si−O−Si stretching and rocking modes, respectively.[37] The intensity of the two bands increased gradually with increasing silica tube content, consistent with the formation of the three-dimensional Si−O−Si network in the hybrid films.[38,39] The broad absorptions around 3200−3700 cm^{-1} were assigned to the Si−OH residue, formed in the hydrolysis of alkoxy groups of APTEOS or TEOS. This band was barely detectable in the spectrum of samples with low silica tube content but clearly noticeable in samples with high silica tube content.

According to the method described in the experimental section, PI−ST hybrid films containing 0, 1, 3, 5, 8, 10, and 20 wt % silica tubes were prepared via in situ polymerization. The silica tubes were combined with DMAc and were sonicated until they were well-dispersed in the liquid. Figure 6 shows the ultraviolet−visible light transmission of PI and PI−ST hybrid films. It can be seen that the transmission decreased in the visible light wave band (380−780 nm) and near-infrared wave band (780−1100 nm) with the increase in silica tube content, and there is no transmission in the UV band (190−380 nm). This was consistent with intuitionistic observation as shown in Figure 7 to demonstrate the optical transparence of the films. The films were quite transparent for hybrids with silica tube loading up to 8 wt %. The films gradually became translucent as the silica tube content was increased further, but they could be still read a letter through the films. The color density also increased with the increase of silica tube content, and the transparency of the hybrid films was closely related to the concentration of the silica tube in the polyimide matrix.

3.3. Cryogenic Mechanical Properties of PI−ST Hybrid Films. As shown in Figure 8, the tensile strength of PI−ST hybrid films at cryogenic temperature was generally higher than that at room temperature. This can be attributed to the tightly packed frozen molecules of polyimide matrix at cryogenic temperature, which lead to a higher tensile strength than that at room temperature. On the other hand, the silica tube−PI matrix interface adhesion was stronger at cryogenic temperature than at room temperature because of the thermal

(37) Kusakabe, K.; Ichike, K.; Hayash, i J. I.; Maeda, H.; Morooka, S. *J. Membr. Sci.* **1996**, *115*, 65.
(38) Morikawa, A.; Iyoku, Y.; Kakimoto, M.; Imai, Y. *Polym. J.* **1992**, *24*, 107.
(39) Srinivasan, S. A.; Hedrick, J. L.; Miller, R. D.; Di, P. R. *Polymer* **1997**, *38*, 3129.

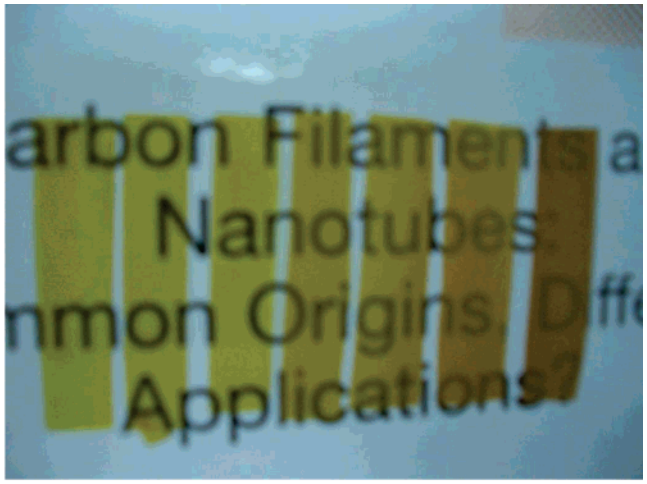

Figure 7. Pictures of PI−ST hybrid films of different silica tube contents (increasing from left to right: 0, 1, 3, 5, 8, 10, and 20 wt %) over a printed paper.

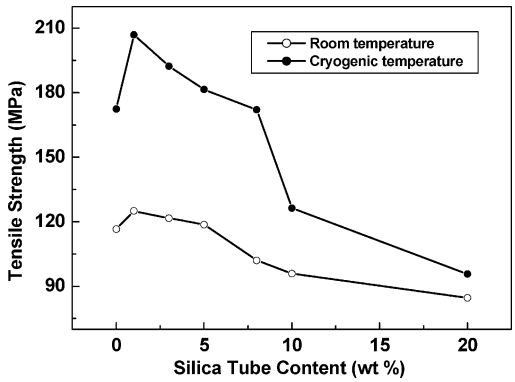

Figure 8. Tensile strength of PI−ST hybrid films at cryogenic and room temperatures.

shrinkage of PI matrix and tight clamping of the silica tube by the PI matrix at cryogenic temperature, leading to a higher composite strength. Figure 8 also shows that the tensile strengths of the hybrid films with 1−5 wt % silica tube were higher than that of the pure PI film at both cryogenic and room temperatures. The tensile strength of the hybrid films exhibited the maximum value at 1 wt % silica tube and then decreased with the increase of silica tube content. The increase in the tensile strength of the PI−ST hybrid films at low silica content could be attributed to the chemical and physical interaction between silica tubes and PI matrix, and the decrease in tensile strength is considered to be caused by the aggregation of silica tube formed in the PI matrix.

Figure 9 shows the tensile modulus of PI−ST hybrid films as a function of silica tube content at cryogenic and room temperatures. It could be seen that the modulus of hybrid films increased monotonically with the increase in silica tube content. This was mainly attributed to the fact that the Young's modulus of the silica tube was much higher than that of the PI matrix and the stretching resistance of the oriented backbone of the polyimide chain contributed to the enhancement of the modulus. Moreover, the modulus at cryogenic temperature was higher than that at room temperature because the modulus of the PI matrix with a tight

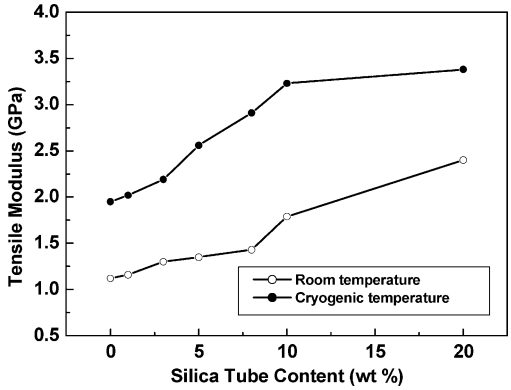

Figure 9. Tensile modulus of PI−silica hybrid films at cryogenic and room temperatures.

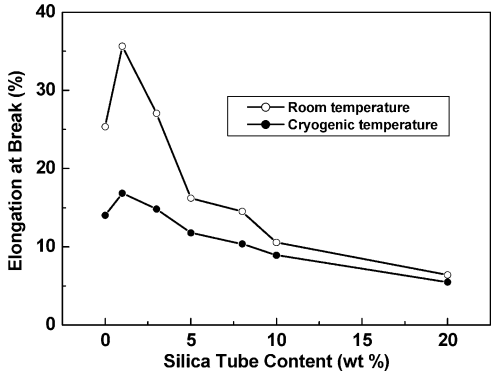

Figure 10. Elongation at break of PI−ST hybrid films at cryogenic and room temperatures.

arrangement at cryogenic temperature was higher than that at room temperature.

Figure 10 showed that the elongation at the break of PI−ST hybrid films was lower at cryogenic temperature than at room temperature and that it was improved with the addition of 1−3 wt % silica tube contents as compared to the pure polyimide film at both cryogenic and room temperatures. This indicated that the strength and ductility of PI hybrid films at 1−3 wt % silica tube contents could be simultaneously increased by the incorporation of amino-modified silica tube. The failure strain of the hybrid films exhibited the maximum value at 1 wt % silica tube, and then decreased with the increase of silica tube content. With the increase of silica tube content, the aggregation will form gradually and result in a decrease in the failure strain of the PI−ST hybrid films. Moreover, it could be observed that the cryogenic failure strain of hybrid films with 1−3 wt % silica tube contents was greater than 15%, showing good ductility at 77 K and usefulness for cryogenic engineering applications. This also indicated that polyimide molecules could undergo deformation at cryogenic temperature though their segmental motion was limited.

3.4. Morphology of the Fracture Surfaces of PI−ST Hybrid Films. Figures 11−14 showed some representative SEM photographs of the PI hybrid films with various silica tube contents. Figure 11 is the SEM photograph of the fracture surface of pure PI film, it can be observed clearly some agglomerative grains, voids and obvious plastic deformed veins, which correspond to shrinkage deformation of the film as a homogeneous material. These microstructure

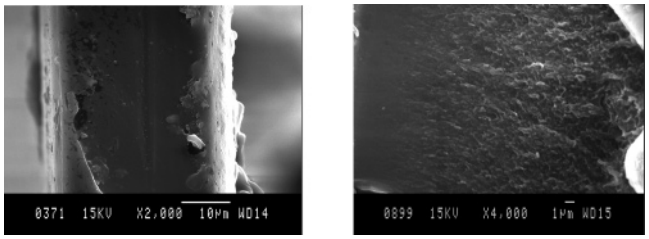

Figure 11. SEM micrographs of fracture surfaces of the pure PI films at room (left, ×1000, scale bar 10 μm) and cryogenic (right, ×1800, scale bar 10 μm) temperatures.

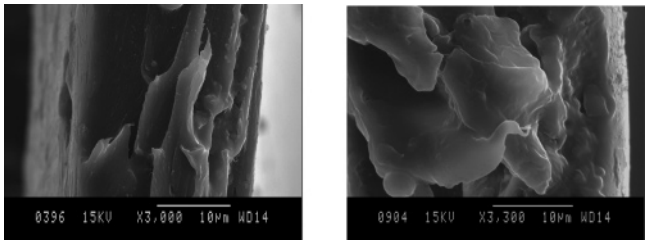

Figure 12. SEM micrographs of fracture surfaces of the PI−ST hybrid film with 1 wt % silica tube at room (left, ×2000, scale bar 5 μm) and cryogenic (right, ×1200, scale bar 10 μm) temperatures.

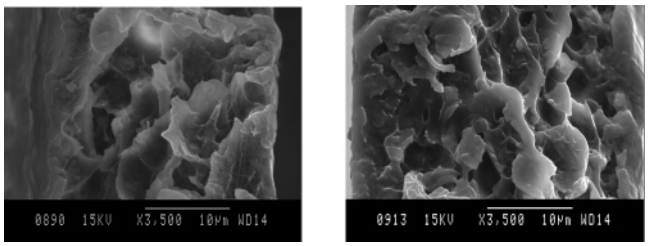

Figure 13. SEM micrographs of fracture surfaces of the PI−ST hybrid film with 10 wt % silica tube at room (left, ×2000, scale bar 5 μm) and cryogenic (right, ×1800, scale bar 10 μm) temperatures.

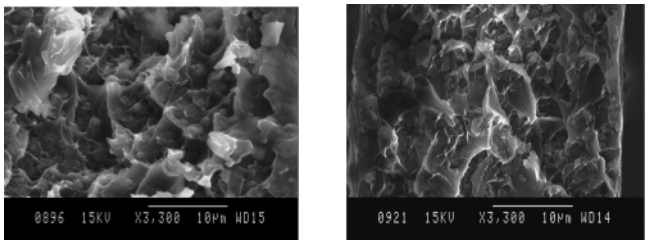

Figure 14. SEM micrographs of fracture surfaces of the PI−ST hybrid film with 20 wt % silica tube at room (left, ×2000, scale bar 5 μm) and cryogenic (right, ×1800, scale bar 10 μm) temperatures.

characteristics generally correspond to lower modulus and strength of the film though it has a better plastic deformation capability. The fracture section in Figure 11 evidenced that the shear failure mode was due to the plastic strain on the fracture surface.

As shown in Figure 12, at low silica tube contents (1 wt %), the morphological change in the fracture sections when silica tubes were added was obvious; there was an enhancement in the tensile strength and ductility of hybrid films as a result of the incorporation and dispersion of silica tube into the matrix. The fracture surfaces of PI−ST films were rougher than those of the pure PI film, indicating that low-content PI−ST hybrid films were more ductile than pure PI film. There were no shrinkage veins but smaller threading dislocation veins in the microscopy range. Few cracks could be found on the fracture section in Figure 12, indicating a delay in the occurrence of microcracking damage and fracture. The relatively high tensile strength and modulus of hybrid films could be attributed partly to the fine microstructures found in the hybrid films. When silica tube content was high such as 10 wt % or more as shown in Figures 13 and 14, large micro- and nanocracks were observed on the fracture surfaces. These cracks were caused mainly by the mismatch of deformation of the two phases in the hybrid film under tension. These cracks would cause a marked drop in the tensile strength and ductility of the hybrid films with higher silica tube contents. Figure 14 gave a micrograph of the region with the plastic veinlike pattern at the edges of film. Microscopically ductile fracture morphology could still be observed at some sites, though the hybrid films with 20 wt % silica tube content exhibited macroscopically brittle behaviors. It had been well-known that the appearance of the fracture surfaces of a polymer composite was closely related to propagation of the crack along the filler (or filler aggregate)−matrix interfaces. For the PI−ST hybrid films with high silica tube contents, the crack would propagate along the silica tube aggregate−PI interfaces, leading to a coarse appearance of the fracture surface. Indeed, quite rough fracture surfaces were observed in Figures 13 and 14 for the PI−ST hybrids with high silica tube contents.

The presence of defects in the microstructure and the adhesion of both the silica tube and the matrix in the hybrid films played a significant role in the reinforcing, stiffening, and toughening of hybrid films. These defects were regarded as a major impediment to obtaining an excellent tensile behavior. Moreover, it was noted that ductile and brittle fracture morphologies for the various silica tube contents could be divided into three different types: without deformation vein pattern (Figure 11), with fine deformation vein pattern (Figure 12), and with bulk deformation vein pattern in microscopy (Figures 13 and 14). The formation of a large number of vein patterns with a fine size of several hundred nanometers could be related to plastic deformation due to the configurations and dense population of hybrids. This was because the smaller nanostructured hybrid films with higher resistance to fracture act as obstacles to cracking. The stress concentration would easily occur in the vicinal zone between the silica tube and the matrix in the hybrid films with a content of 10 wt % or more silica tube. In addition, Figures 11−14 showed that the fracture surfaces of the hybrid films were rougher at room temperature than those at cryogenic temperature, indicating that the fractures at cryogenic temperature were more brittle than those at room temperature, leading to a reduction in ductility of hybrid films compared with those at room temperature.

3.5. Dynamic Mechanical Properties of PI−ST Hybrid Films. Figure 15 showed the dynamic mechanical analysis (DMA) curves, which was the storage modulus of the PI−ST hybrid films as a function of temperature from −150 to 500 °C. Clear differences in the storage modulus were shown among the films with different silica tube contents. The dynamic mechanical behavior of the hybrid films indicated that the films with higher silica tube contents exhibited higher storage modulus values than those of lower silica tube

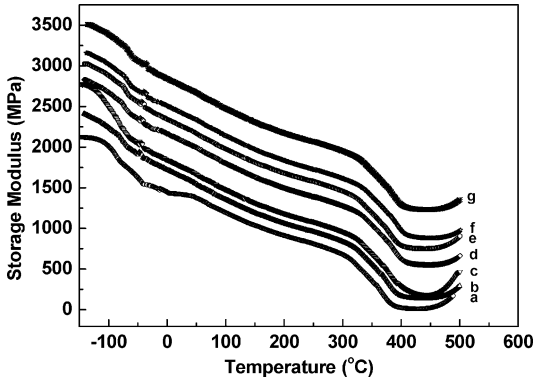

Figure 15. Effect of temperature on the storage modulus of PI−ST hybrid films. The silica tube content: (a) 0 % ST and (b) 1, (c) 3, (d) 5, (e) 8, (f) 10, and (g) 20 wt %.

contents. For each sample, the storage modulus decreased with an increase in temperature from −150 °C to about 420 °C and then increased slightly. The minimum of storage modulus occurred at around 406−426 °C for various samples, and increased with the increase in silica tube content. The glass-transition temperature (T_g) was determined by the minimum value of the plots of storage modulus vs temperature for the hybrid films. The T_g values are 406, 408, 409, 412, 415, 419, and 426 °C for the 0 (unfilled), 1, 3, 5, 8, 10, and 20 wt % PI−ST hybrid films, respectively. The experimental results indicated that the PI−ST hybrid films possessed higher glass-transition temperatures compared to the pure polyimide, and the incorporation of silica tubes could improve the thermal stability of th polyimide film. These results were similar to those reported on addition of single-walled and multiwalled carbon nanotubes to polyimide.[21,40] These results also indicated that there was significant interaction between the polyimide and the silica tube.

4. Conclusion

The polyimide−silica tube hybrid films were prepared via ultrasonic dispersion and an in situ polymerization process. The silica tubes were synthesized by template self-assembly from D,L-tartaric acid and hydrolysis of tetraethyl orthosilicate (TEOS), and their surfaces were modified by 3-aminopropyltriethoxysilane coupling agent. The prepared hybrid films had higher strength and modulus at cryogenic temperature than those at room temperature, and their strength, modulus, and failure strain could be simultaneously increased compared to the pure PI film when the silica tube was at 1−3 wt %. The cryogenic failure strain of hybrid films with 1−3 wt % silica tube contents was >15%, revealing good ductility at 77 K. The glass-transition temperature of hybrid films was also improved with the incorporation of silica tube. The improved properties of the novel PI−ST hybrid films show good potential for employment in superconductive insulating and other cryogenic applications.

Acknowledgment. This work is supported by the Key Project of Chinese Ministry of Education (107023); the Postdoctoral Fellowship Scheme of The Hong Kong Polytechnic University (Account G-YX70) and the Fund of China University of Geosciences (Beijing) (51900903001).

CM062540M

(40) Ogasawara, T.; Ishida, Y.; Ishikawa, T.; Yokota, R. *Composites, Part A* **2004**, *35*, 67.